

Impact of Obesity on Postprandial Triglyceride Contribution to Glucose Homeostasis, Assessed with a Semimechanistic Model

Jennifer Leohr^{1,*} and Maria C. Kjellsson²

The integrated glucose-insulin model is a semimechanistic model describing glucose and insulin after a glucose challenge. Similarly, a semiphysiologic model of the postprandial triglyceride (TG) response in chylomicrons and VLDL-V6 was recently published. We have developed the triglyceride-insulin-glucose-GLP-1 (TIGG) model by integrating these models and active GLP-1. The aim was to characterize, using the TIGG model, the postprandial response over 13 hours following a high-fat meal in 3 study populations based on body mass index categories: lean, obese, and very obese. Differential glucose and lipid regulation were observed between the lean population and obese or very obese populations. A population comparison revealed further that fasting glucose and insulin were elevated in obese and very obese when compared with lean; and euglycemia was achieved at different times postmeal between the obese and very obese populations. Postprandial insulin was incrementally elevated in the obese and very obese populations compared with lean. Postprandial chylomicrons TGs were similar across populations, whereas the postprandial TGs in VLDL-V6 were increased in the obese and very obese populations compared with lean. Postprandial active GLP-1 was diminished in the very obese population compared with lean or obese. The TIGG model described the response following a high-fat meal in individuals who are lean, obese, and very obese and provided insight into the possible regulation of glucose homeostasis in the extended period after the meal by utilizing lipids. The TIGG-model is the first model to integrate glucose and insulin regulation, incretin effect, and postprandial TGs response in chylomicrons and VLDL-V6.

Study Highlights

WHAT IS THE CURRENT KNOWLEDGE ON THE TOPIC?

☑ The interplay between glucose homeostasis and lipid regulation in healthy lean individuals has been characterized. However, the regulation within obesity is not well-established.

WHAT QUESTION DID THIS STUDY ADDRESS?

☑ We quantitatively characterized the postprandial response of glucose, insulin, active GLP-1, and triglycerides over 13 hours following a high-fat meal in individuals who are lean, obese, and very obese.

WHAT DOES THIS STUDY ADD TO OUR KNOWLEDGE?

☑ We developed the triglyceride-insulin-glucose-GLP-1 (TIGG) model; the first model to integrate the glucose and

insulin regulation, incretin effect, along with postprandial triglycerides (TGs) response in a semimechanistic way. It elucidated the important aspects of TG contribution to glucose homeostasis.

HOW MIGHT THIS CHANGE CLINICAL PHARMACOLOGY OR TRANSLATIONAL SCIENCE?

☑ These findings would be of significant interest to those studying lipids, incretins, and metabolic pathways especially in relation to pharmacological interventions against obesity and in type 2 diabetes. Additionally, the TIGG model provides a useful tool for others in the field to aid understanding of these complex relationships and for design of future clinical studies.

Obesity is recognized as a major health epidemic worldwide for which cardiovascular morbidity and mortality remains the leading cause of death.¹ Increased adiposity is often associated with metabolic syndrome, which is characterized by increased insulin resistance with dyslipidemia (increased triglycerides (TGs), and low-density lipoprotein cholesterol, with decreased high-density

lipoprotein cholesterol).² It has been well-established that there is a balance among glucose, insulin, and lipid regulation within metabolism that is altered with obesity.³

Mathematical models are powerful tools to characterize the complex relationships within metabolism. The application of models within diabetes research is well-established and has increased

¹Department of Pharmacokinetics/Pharmacodynamics, Lilly Research Laboratories, Lilly Corporate Center, Indianapolis, Indiana, USA;

²Pharmacometrics Research Group, Department of Pharmacy, Uppsala University, Uppsala, Sweden. *Correspondence: Jennifer Leohr (Leohr_Jennifer_K@lilly.com)

Received November 8, 2021; accepted March 16, 2022. doi:10.1002/cpt.2604

understanding of the complex interplay between glucose and insulin. The integrated glucose-insulin model (IGI) is a semimechanistic model that describes glucose homeostasis⁴ and has supported several clinical trials.^{5–7} However, major regulators of metabolism, such as lipids, have not been incorporated in the IGI model. Beyond the glucose utilized for maintaining the energy needs, lipid oxidation from free fatty acids (FFAs) contributes 90% of the muscle energy requirements at rest.^{8,9} Recently, a semiphysiologic lipokinetic model was developed describing the absorption of TGs after a high-fat meal and compared the dynamics of TGs in chylomicrons and large very low-density lipoprotein-V6 particles (VLDL-V6) in individuals who are lean, obese, and very obese.¹⁰ The TGs in VLDL-V6 represent 80% of the postprandial response of total TGs after a high-fat meal. Furthermore, the postprandial TGs response of VLDL-V6 differed between individuals who are lean and obese. Likewise, others have found that most of the postprandial TG response is represented in VLDL,¹¹ and larger VLDL may be more influential in metabolic syndrome,¹² insulin sensitivity, obesity, and weight regulation.

The interplay of insulin, glucose, and lipids is further complicated during the postprandial state where the body responds to nutrients in the gut via incretins which have been found to be important in the development of diabetes.¹³

The objective of this work was to characterize, using an integrated semimechanistic model, the postprandial response of TGs, glucose, insulin, and active glucagon-like peptide 1 (GLP-1) after consuming a high-fat meal. Additionally, this model was used to investigate differences between individuals who are lean to individuals who are obese.

METHODS

Clinical study

This was a single center study approved by the Indiana University Institutional Review Board in 2006. All participants gave written informed consent. Study procedures were performed in accordance with the ethical standards of the institutional and/or national research committee and with the 1964 Helsinki declaration and its later amendments or comparable ethical standards. Public trial registration was not required at the time of the trial.

Study design

Sixty-four individuals, 31 men and 33 women, age 26–45 years, with no known cardiometabolic disease, drug dependency, not taking essential medication or dietary supplements, or without weight loss >5 kg in the last 6 months participated in the study. Participants were categorized into three study populations based on their body mass index (BMI): lean (BMI 18.5–24.9), obese (BMI 30–33), and very obese (BMI 34–40). Demographics by study population is presented in **Table 1**.

Key exclusion criteria were individuals who have a recent history (within 1 year) of cardiovascular, respiratory, hepatic, renal, gastrointestinal, endocrine, hematological, or neurological disorders capable of significantly altering the study procedures or interfering with the data interpretation. Individuals with fasting TGs >400 mg/dL were excluded.

On day 1, participants were given the same standardized meal for breakfast, lunch, and dinner. Participants were then fasted overnight, and a high-fat meal was served containing 660 kcal, with 60% fat (~75% unsaturated/25% saturated fat), 20% protein, and 20% carbohydrates and consumed entirely within 20 minutes. The purpose of this meal was to induce a postprandial hyperlipidemia.¹⁴ Blood samples were taken prior to the high-fat meal (fasted) and 4-, 7-, 10-, and 13-hours postmeal, for determination of glucose, active

Table 1 Population characteristics

Study population	Age (years)	BMI (kg/m ²)	Fat (%)	WT (kg)	HC (cm)	WC (cm)	FPG (mg/dL)	HbA1c (%)	HOMA-IR
Lean	Mean	22.7	10.6	70.4	96.2	80.0	95.5	5.28	0.41
N = 24	95% CI	22.1;23.4	7.83;13.3	67.0;73.7	93.7;98.8	77.6;82.3	92.1;99.0	5.13;5.42	0.27;0.55
Obese	Mean	31.8	32.0	89.0	112	98.9	101	5.45	0.75
N = 23	95% CI	31.3;32.3	29.2;34.8	85.3;85.3	110;114	96.0;102	97.2;105	5.29;5.61	0.60;0.89
Very obese	Mean	36.6	40.6	107	120	116	104	5.69	1.63
N = 17	95% CI	35.7;37.4	37.4;43.7	101;113	118;123	112;119	99.5;108	5.51;5.88	1.23;2.03

Abbreviations: BMI, body mass index; Fat, body fat; FPG, fasting plasma glucose (mg/dL); HbA1c, glycated hemoglobin; HC, hip circumference; HOMA, homeostasis model assessment for insulin resistance; HOMA-IR; WC, waist circumference; WT, weight.

GLP-1, insulin, glucagon, and lipids. No additional food intake, apart from water, was allowed during the blood sampling period.

Determination of biomarkers

Glucose. Plasma glucose was analyzed using a validated assay (Covance, IN) with an interassay precision and accuracy of $\leq 1.1\%$. The lower and upper limit of quantification was 20 mg/dL and 16,000 mg/dL, respectively.

Active GLP-1, insulin, and glucagon. Plasma was collected for active GLP-1, glucagon, and insulin using P100 tubes containing a cocktail of protease inhibitors, specifically optimized for stabilization of metabolic markers. Active GLP-1, glucagon, and insulin were analyzed using a validated immunoassay method (Myriad RBM, Inc., Austin, TX) with an interassay precision and accuracy of active GLP-1, and insulin of $\leq 12\%$ and $\leq 20\%$ for glucagon. The lower limit of quantification and upper limit of quantification was 0.0281 $\mu\text{U/mL}$ and 140 $\mu\text{U/mL}$ for insulin, 4.38 pg/mL and 2,200 pg/mL for active GLP-1, and 3.0 pg/mL and 15,000 pg/mL for glucagon, respectively.

Lipids. Plasma was analyzed for TG content in chylomicrons (≥ 170 nm), VLDL-V6 particles (VLDL-V6, 140–100 nm) using nuclear magnetic resonance signals, broadcast by lipoprotein subclass particles of different sizes (LipoScience, Raleigh, NC).¹⁵

Statistical testing of observed data

The incremental area under the curve (iAUC) of the change in concentration from baseline (i.e., fasting) vs. time curve was calculated by study population (lean, obese, and very obese) for glucose, insulin, active GLP-1, glucagon, TGs in chylomicrons, and TGs in VLDL-V6. Statistical tests of the observed data were performed on the fasting concentration or iAUC among individuals who are lean versus obese, lean versus very obese, and lean vs. all obese (obese and very obese). A one-sided *t*-test was used, assuming normally distributed variables. The statistical tests were hypothesis generating for the model development.

Model development

Published IGI, GLP-1, and lipokinetic models were used as a starting point for the triglyceride-insulin-glucose-GLP-1 (TIGG) model. Each submodel is described below, along with highlighted differences in implementation taken from the start of the model development. For the initial development step, the structure and parameters were fixed to what was reported in the original publications, except for those changes mentioned below and residual errors. Parameters were then allowed to be estimated and structural changes were explored, where model misspecifications were indicated. A parsimonious approach was taken in an attempt to conserve structures and parameters from previous publications.

Glucose and insulin submodel. The IGI model developed for intravenous glucose tolerance test by Silber *et al.*⁴ and for an oral glucose tolerance test by Jauslin *et al.*¹⁶ was used as the initial model for the glucose and insulin submodels. It includes a two-compartment disposition model for glucose, with a first order insulin-independent and a first order insulin-dependent elimination; a one-compartment disposition model for insulin with a first order elimination; and two feedback mechanisms between glucose and insulin: glucose stimulates insulin secretion and insulin stimulates glucose elimination. Calculations of the endogenous glucose production and basal insulin secretion assumes that baseline measurements reflect steady-state. Glucose absorption is described with a two-compartment transit absorption model where absorption rate constant and mean transit time is estimated.

The incretin effect, greater insulin response after oral glucose compared with intravenous glucose, in the IGI model was replaced by a

stimulatory effect (linear or maximum effect (E_{max})) of measured active GLP-1 on insulin secretion.

GLP-1 submodel. Active GLP-1 is released upon stimulation by intestinal glucose and lipids¹⁷ and is rapidly degraded to inactive GLP-1. As the first postmeal sample in this study was taken 4 hours after the high-fat meal, the glucose stimulation of GLP-1 was assumed to be negligible. Active GLP-1 was modeled using a turnover model, fixing the elimination half-life to 2 minutes¹⁸ and the lipid-related stimulation was investigated.

Triglyceride submodel. The TG data of this study has previously been reported along with development of a semiphysiologic lipokinetic model.¹⁰ This lipokinetic model describes the absorption of TGs from dietary fats in the gut via chylomicrons and the postprandial VLDL secretion from the liver as VLDL-V6.¹⁰

Parameter estimates and model-based statistical analysis

Nonlinear mixed-effect modeling was used to analyze the data, using NONMEM¹⁹ (version VII) and Perl-speaks-NONMEM (PsN)²⁰ as the modeling environment. The first-order conditional estimation method with interaction was used. The model was implemented as ordinary differential equations using the ADVAN6 subroutine.

Selection between models was based on visual inspection of goodness-of-fit plots, including conditional weighted residuals,²¹ visual predictive checks (VPCs), the objective function value (OFV), the physiological plausibility, and precision of parameter estimates. The likelihood ratio test was used between nested models, assuming the difference in OFV is χ^2 -distributed with the number of differing parameters being the degree of freedom and *P* value = 0.01 for statistical significance.

The final model was evaluated using internal validation methods. The quantified between-subject variability was expressed as a coefficient of variation. Sampling Importance Resampling was performed to assess the uncertainty in the parameter estimates using PsN and reported as relative standard error (RSE (%)) and 90% confidence interval (CI).²⁰ The predictive properties of the model were evaluated by performing VPCs using PsN and Xpose in R.²² The VPC was performed by simulating 1000 study replicates with the realized study design of the original study. At each observation time point, the 10th, 50th, and 90th percentiles of glucose, insulin, active GLP-1, chylomicrons, and VLDL-V6 were calculated for each study replicate. The 95% CIs of these percentiles were then calculated and plotted over time, with percentiles calculated from the observed data overlaid. As the number of individuals in each weight group was limited, a lower prediction interval (PI) was investigated (i.e., 80% PI instead of 95% PI).

RESULTS

Study results of observed clinical data

Triglycerides. As previously described, the fasting TG concentrations of chylomicrons and VLDL-V6 were similar among the lean, obese, and very obese populations (Table 2).¹⁰ The TGs in chylomicrons (Figure 1a) and large VLDL-V6 (Figure 1b) both increased postprandially. The iAUC of the TGs in chylomicron was not statistically different between the populations. However, the iAUC of the TG in VLDL-V6 was significantly greater in obese or very obese population ($P < 0.02$) compared with lean.

Glucose. Fasting glucose concentrations were elevated in the obese and very obese population compared with the lean (Table 2, Figure 1c). No postprandial glucose increase was

Table 2 Statistical analysis of fasting concentrations and iAUC of chylomicron TG, VLDL-V6 TG, glucose, insulin, active GLP-1, and glucagon in three investigated populations

	N	Fasting			Postprandial response iAUC			
		Mean, mg/dL	Ratio	P value	Mean, mg*hour/dL	Ratio	P value	
Chylomicron TGs								
Lean	24	3.35			69			
Obese	23	3.67	1.10	0.53 ^a	75	1.09	0.34 ^a	
Very obese	17	3.22	0.96	0.80 ^b	71	1.03	0.45 ^b	0.37 ^c
VLDL-V6 TGs								
Lean	24	6.31			340			
Obese	23	3.13	0.50	0.05 ^a	505	1.49	0.01 ^a	
Very obese	17	6.64	1.05	0.90 ^b	445	1.31	0.08 ^b	0.02 ^c
	N	Mean, pg/mL	Ratio	P value	Mean, pg*hour/mL	Ratio	P value	
Glucose								
Lean	24	95.2			-22.4			
Obese	23	99.5	1.05	0.08 ^a	-78.8	3.51	0.02 ^a	
Very obese	17	105	1.09	<0.01 ^b	-76.3	3.40	0.03 ^b	0.005 ^c
	N	Mean, uIU/mL	Ratio	P value	Mean, uIU*hour/mL	Ratio	P value	
Insulin								
Lean	24	1.30			48.5			
Obese	23	2.64	2.03	<0.01 ^a	57.9	1.19	0.12 ^a	
Very obese	17	5.19	3.99	<0.01 ^b	62.9	1.30	0.06 ^b	0.48 ^c
	N	Mean, pg/mL	Ratio	P value	Mean, pg*hour/mL	Ratio	P value	
Active GLP-1								
Lean	24	25.7			526			
Obese	23	25.7	0.99	0.96 ^a	541	1.03	0.67 ^a	
Very obese	17	25.0	0.97	0.83 ^b	448	0.85	0.02 ^b	<0.01 ^c
Glucagon								
Lean	24	94.2			1,143			
Obese	23	45.9	0.48	0.02 ^a	1,311	1.14	0.31 ^a	
Very obese	17	149	1.58	0.15 ^b	1,101	0.96	0.78 ^b	0.25 ^c

Abbreviations: iAUC, area under the curve of the change from baseline; TGs, triglycerides.

^aP value represents statistical analysis between lean and obese population. ^bP value represents statistical analysis between lean and very obese population.

^cP value represents statistical analysis between lean and all obese population.

observed, likely due to the lack of sampling between 0- and 4 hours postmeal. Mean glucose concentration remained flat and euglycemic for the entire collected 13-hour assessment period in the lean population. In the obese population, the elevated fasting glucose was diminished 4 hours postmeal and maintained for the remainder of the assessment period. Fasting glucose concentrations were the highest in the very obese population and reduced during the entire 13-hour assessment period. At 10–13 hours postmeal, the glucose concentration was similar to the lean and obese population.

Insulin. Fasting insulin concentrations were significantly elevated in the obese or very obese population (both, $P < 0.01$) compared with the lean (Table 2, Figure 1d). Peak insulin levels were

observed 4 hours postmeal and were incrementally increased by populations. The insulin iAUC was greater in the obese or very obese population compared to the lean (Table 2).

Active GLP-1. Fasting active GLP-1 concentrations were similar across the study populations. Peak active GLP-1 concentrations were observed 4 hours postmeal in all populations. The active GLP-1 concentration time profile was similar in the lean or obese populations; whereas, the active GLP-1 iAUC was significantly lower in the very obese population ($P = 0.02$).

Glucagon. Fasting glucagon concentrations were significantly elevated in the very obese compared with the obese or lean populations (Table 2, Figure 1f); however, there was no

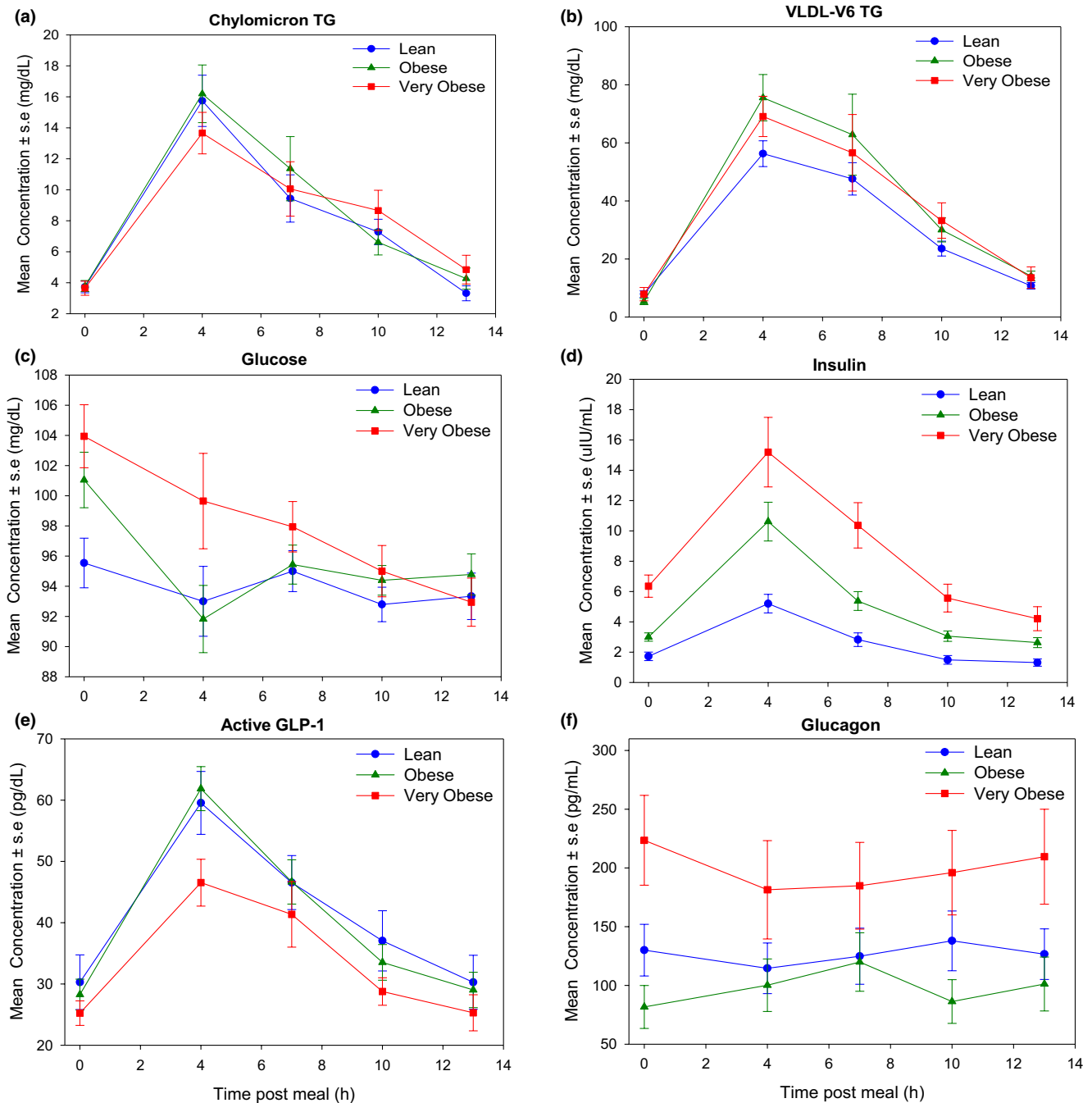


Figure 1 Mean concentration (\pm standard error) vs. time of (a) chylomicron TG, (b) VLDL-V6 TG, (c) glucose, (d) insulin, (e) active GLP-1, and (f) glucagon following a high-fat meal in individuals who are lean (blue), obese (green), and very obese (red). Abbreviation: TG, triglycerides. [Colour figure can be viewed at wileyonlinelibrary.com]

postprandial response. The concentrations remained generally flat for the entire collected assessment period for all populations.

The TIGG Model

Triglyceride submodel. As the published lipokinetic model was developed from the TG data of this study, the model structure was not altered, and the model parameters were fixed. This model consisted of two transit compartments describing fat absorption and two central compartments for the chylomicron and VLDL-V6.

GLP-1 submodel. The elimination rate constant, $k_{out, GLP-1}$ was fixed to $\ln(2)/2$ minutes (i.e., fixing the half-life of active GLP-1 to 2 minutes) and, ignoring the stimulation of glucose on the production, assumed that the fasting active GLP-1 concentrations collected at time = 0 were at steady-state, thus:

$$GLP_{SS} = \frac{k_{in, GLP-1}}{k_{out, GLP-1}} \iff k_{in, GLP-1} = GLP_{SS} \cdot k_{out, GLP-1} \quad (1)$$

The effect of the transit compartments for the fat absorption, chylomicrons, or VLDL-V6 were explored on production of active GLP-1 using either an E_{\max} or a linear model. The lowest OFV was observed with the TGs in the second transit compartment using a linear relationship.

$$dGLP1/dt = k_{in,GLP-1} + \alpha_{GLP1} \cdot TG_{tr2} - k_{out,GLP-1} \cdot GLP1 \quad (2)$$

where TG_{tr2} is TG amount in the second transit compartment of the fat absorption and α_{GLP-1} is the slope of the relationship. Different α_{GLP-1} for each study population (lean, obese, and very obese) was investigated in the model; however, no statistically improvement was observed.

Insulin submodel. The parameter for insulin clearance ($CL_I = 73.2$ L/hour) and central volume ($V_I = 6.09$ L) reported by Jauslin *et al.*²³ were used to calculate the $k_{out,INS} = 12$ /hours. The model assumed that the fasting insulin concentrations collected at time = 0 were at steady-state, thus:

$$I_{SS} = \frac{k_{in,INS}}{k_{out,INS}} \iff k_{in,INS} = I_{SS} \cdot \frac{CL_I}{V_I} \quad (3)$$

This assumption seemed appropriate as insulin concentration at the end of the sampling period (13 hours) was similar to the insulin concentration at time 0 (fasting levels; **Figure 1d**). As fasting insulin concentrations differed by study population, I_{ss} was estimated separately for each population ($I_{SS,Lean}$, $I_{SS,Obese}$, and $I_{SS,VeryObese}$).

The incretin effect of active GLP-1 on insulin secretion was evaluated as a linear or E_{\max} function on $k_{in,INS}$. The linear function and E_{\max} had the same OFV, thus the smaller linear function was used.

$$dINS/dt = k_{in,INS} + Incretin - k_{out,INS} \cdot INS \quad (4)$$

$$Incretin = \alpha_{INS} \cdot (GLP1(t) - GLP1_{SS}) \quad (5)$$

where $GLP1_{SS}$ is GLP-1 concentration at baseline (fasting), or steady-state, and α_{INS} is the slope of the relationship between the change from baseline active GLP-1 concentrations and the $k_{in,INS}$.

Glucose submodel. The following parameters were fixed from previous publications: absorption rate constant ($k_{a,G} = 0.906$ /hour), insulin-dependent glucose clearance ($CL_{GI} = 0.497$ L/hour \cdot mL/ μ U), and central volume ($V_G = 9.33$ L), as reported by Jauslin *et al.*¹⁶ and insulin-independent clearance for healthy individuals ($CL_G = 5.36$ L/hour or 0.0894 L/min), as reported by Alskär *et al.*²⁴ The disposition was reduced from a two-compartment model to a one-compartment model without deterioration in fit (i.e., the same OFV).

As fasting glucose concentrations differ among the three populations, the baseline glucose was estimated separately for each population: $G_{Base,Lean}$, $G_{Base,Obese}$ and $G_{Base,VeryObese}$.

This elevated glucose has been reported to be associated with primarily a decrease in peripheral glucose disposal.²⁵ Due to this, insulin-dependent glucose clearance for the obese and very obese

populations was estimated based on the relative ratio to the lean population.

$$CL_{GI,Obese} = CL_{GI,Lean} \cdot I_{SS,Lean}/I_{SS,Obese} \quad (6)$$

$$CL_{GI,VeryObese} = CL_{GI,Lean} \cdot I_{SS,Lean}/I_{SS,VeryObese} \quad (7)$$

The assumption of steady-state within the turnover model for glucose seemed appropriate for the lean population, as the glucose concentrations at the end of the assessment period were similar to fasting glucose concentrations (baseline; **Figure 1c**). Thus, is the same as $G_{Base,Lean}$. However, this assumption was not appropriate for the obese or very obese populations, as fasting glucose concentration differed from the concentrations 13 hours later. To address this within the model, a calculation of the half-life based on the rate of endogenous glucose production was used.

The rate of glucose production, EGP_{SS} , was related to the insulin-dependent glucose clearance (CL_{GI}), the insulin independent glucose clearance (CL_G), and the ratio:

$$EGP_{SS} = (CL_{GI} \cdot I_{SS} + CL_G) \cdot G_{Base,Lean} \cdot \left(1 - \text{Ratio} \cdot e^{-\frac{\ln(2)}{t_{1/2}} \cdot t}\right) \quad (8)$$

$$\text{Ratio}_{Lean} = \frac{G_{Base,Lean} - G_{Base,Lean}}{G_{Base,Lean}} = 0 \quad (9)$$

$$\text{Ratio}_{Obese} = \frac{G_{Base,Obese} - G_{Base,Lean}}{G_{Base,Lean}} \quad (10)$$

$$\text{Ratio}_{VeryObese} = \frac{G_{Base,VeryObese} - G_{Base,Lean}}{G_{Base,Lean}} \quad (11)$$

Thus, the change of glucose over time was defined as:

$$d\text{Glucose}/dt = EGP_{SS} - (CL_{GI} \cdot I_E + CL_G) \cdot \text{Glucose} \quad (12)$$

Using the published parameters of CL_{GI} and CL_G , the model was able to reflect the glucose response in the obese and very obese populations but there was a misfit for the lean population (**Figure 2**, top panels). The model predicted a reduction in the glucose profile due to the increase in postprandial insulin. However, observed glucose levels remained flat in the lean population for the entire collected assessment period, indicating a contribution of another energy source. To assess this within the model, the postprandial TG response of chylomicron or VLDL-V6 was added to endogenous glucose production. The best model fit was observed with the TGs in VLDL-V6. When adding an effect for an increase in the endogenous glucose production, the model was improved (Δ OFV = -134) and reflected the observed data (**Figure 2**, bottom panels).

$$d\text{Glucose}/dt = EGP_{SS} + f(\text{VLDL}) - (CL_{GI} \cdot I_E + CL_G) \cdot \text{Glucose} \quad (13)$$

$$f(\text{VLDL}) = \alpha_G \cdot (\text{VLDL} - V6(t) - \text{VLDL} - V6_{SS}) \quad (14)$$

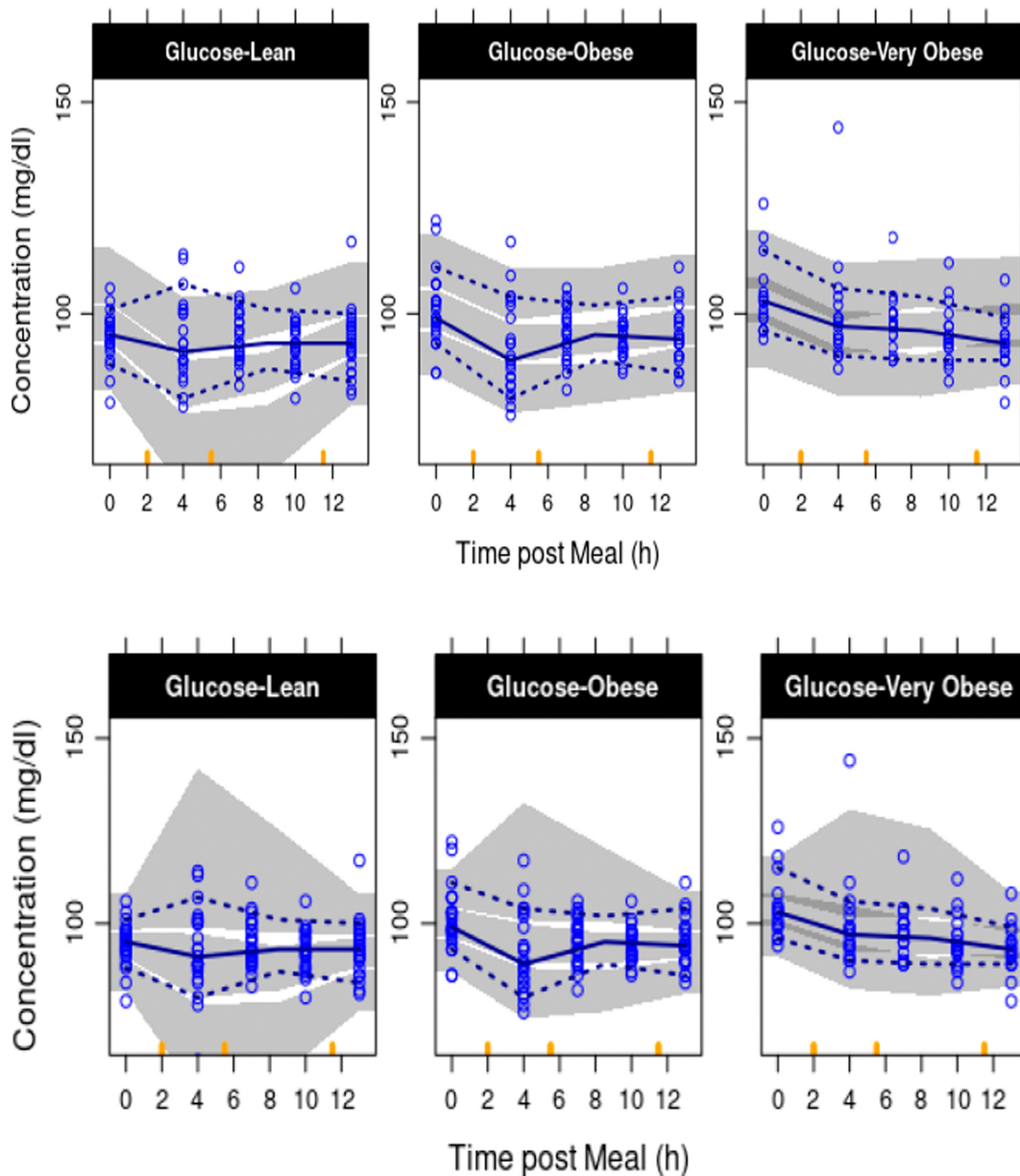


Figure 2 Visual predictive check of the model predictions of glucose concentration for the three investigated populations lean (left column), obese (middle column), and very obese (right column) for model without endogenous glucose production (top row) and after adding endogenous glucose production (bottom panel). The blue symbols are observation related: dots are observations, solid line is median and dashed line is the 10th and 90th percentile of data. The grey shaded area represents the 80% confidence interval of the 10th, 50th, and 90th percentiles of model simulations. [Colour figure can be viewed at wileyonlinelibrary.com]

where $VLDL-V6_{ss}$ is VLDL-V6 TG concentration at baseline (fasting), or steady-state, and α_G is the slope of the relationship between the change from baseline VLDL-V6 concentrations and the EGP_{ss} .

Additionally, α_G was separately estimated for the lean and obese (combining obese and very obese) populations which improved the fit of the model ($\Delta OFV = -8$).

Parameter and model evaluation. Table 3 lists the parameter estimates of the TIGG model and the corresponding 90% CIs obtained from the Sampling Importance Resampling. The RSEs for fixed-effects parameters were all <41%, indicating that the

parameters were reasonably well-estimated, except for the rate constant for the removal of $EGP_{t1/2}$ (RSE = 51%). Figure 3 shows the VPC corresponding to the response following the high-fat meal and the model predictions where both the typical profiles and variability in data were adequately captured by the model. Figure 4 presents a schematic representation of the TIGG model. The equations of the model are included in **Supplementary Information**.

DISCUSSION

The current clinical study investigated the response of glucose, insulin, active GLP-1, glucagon, TGs in chylomicrons, and VLDL-V6 following a high-fat test meal in individuals who are lean, obese,

Table 3 Final parameter estimates, typical value, and BSV, with uncertainty represented as RSE and 90% CI of estimates from an SIR analysis

Parameter description	Parameter	Unit	Typical value [RSE; 90% CI ^a]	BSV [RSE, 90% CI ^a]
Glucose-insulin system estimates				
Glucose absorption rate constant ^b	$k_{a,G}$	1/hour	0.906	-
Insulin dependent glucose clearance ^b for lean	CL_{GI}	L/hour·mL/μU	0.497	-
Insulin independent glucose clearance ^b	CL_G	L/hour	5.36	-
Volume of distribution of glucose ^b	V_G	L	9.33	-
Baseline glucose in lean population	$G_{Base, Lean}$	mg/dL	94.2 [0.85; 92.6–95.7]	5.36 [16.5; 4.50–6.01] ^c
Baseline glucose in obese population	$G_{Base, Obese}$	mg/dL	101 [1.33; 98.0–104]	5.36 [16.5; 4.50–6.01] ^c
Baseline glucose in very obese population	$G_{Base, Very Obese}$	mg/dL	103 [1.47; 99.3–106]	5.36 [16.5; 4.50–6.01] ^c
Half-life of endogenous glucose production	$EGP_{t1/2}$	hour	0.150 [51.3; 0.047–0.39]	
Elimination rate constant of insulin ^b	$k_{out,INS}$	L/hour	12	-
Volume of distribution of insulin ^b	V_{INS}	L	6.09	-
Rate constant for insulin delay ^b	k_{IE}	L/hour	0.464	-
Baseline insulin in lean population	$I_{SS, Lean}$	μU/mL	1.01 [13.7; 0.753–1.31]	68.8 [23.5; 57.6–83.5] ^c
Baseline insulin in obese population	$I_{SS, Obese}$	μU/mL	2.06 [13.2; 1.57–2.65]	68.8 [23.5; 57.6–83.5] ^c
Baseline insulin in very obese population	$I_{SS, Very Obese}$	μU/mL	4.35 [15.6; 3.14–6.19]	68.8 [23.5; 57.6–83.5] ^c
Slope of incretin effect	α_{INS}		1.68 [10.5; 1.29–2.23]	
Slope of VLDL-V6 TG effect on $EGP_{SS,G}$ for lean	$\alpha_{G,Lean}$		10.13 [20.5; 6.36–15.5]	
Slope of VLDL-V6 TG effect on $EGP_{SS,G}$ for obese and very obese	$\alpha_{G,Obese}$		4.38 [24; 2.65–6.21]	
Residual error of glucose	RES_G	%	5.33 [10.2; 4.79–5.81]	
Residual error of insulin	RES_{INS}	%	43.3 [10.5; 38.8–49.3]	
Lipid system estimates				
Triglyceride absorption rate constant ^b	$k_{a,TG}$	1/hour	0.606	-
Volume of chylomicrons and VLDL-V6 ^b	V_{lipids}	L	8.44	28
Baseline chylomicrons ^b	CHY_{SS}	mg	28.7	29
Transfer rate constant from Chylo to VLDL-V6 ^{b,d}	k_{tra}	1/hour	11.6	25
Removal rate constant of VLDL-V6 ^b	$k_{out,V}$	1/hour	2.23	31
Baseline VLDL-V6 ^b	$VLDL-V6_{SS}$	mg	49	43
Effect of HOMA on k_{tra} ^c	EFF_{HOMA}		0.183	-
Residual error of chylomicrons	RES_{CHO}	%	48.3 [9.67; 43.9–54.3]	
Residual error of VLDL-V6	RES_{VLDL}	%	48.8 [10.7; 43.7–54.8]	
Incretin system estimates				
Elimination rate constant of active GLP-1	$k_{out,GLP1}$	1/hour	20.8	39 [24.0; 30.2–46.1]

(Continued)

Table 3 (Continued)

Parameter description	Parameter	Unit	Typical value [RSE; 90% CI ^a]	BSV [RSE, 90% CI ^a]
Baseline active GLP-1	GLP1 _{SS}	pg/mL	24.3 [5.30; 21.7–27.0]	40 [20.4; 33.5–46.3]
Slope of on $k_{in, GLP-1}$	α_{GLP-1}		0.356 [6.26; 0.305–0.415]	
Residual error of active GLP-1	RES _{GLP1}	%	22.1 [10.5; 20.0–24.5]	

Abbreviations: BSV, between subject variability; CI, confidence interval; HOMA, homeostasis model assessment for insulin resistance; RSE, relative standard error; SIR, Sampling Importance Resampling; TG, triglyceride.

^aDerived from sampling importance resampling. ^bParameter fixed to value reported in original publication. ^cBSV shared between population.

^d $k_{tra} = k_{tra} \cdot \left(\frac{HOMA_i}{HOMA_{lean}} \right)^{EFF_{HOMA}} \cdot e^{\eta_i}$, where HOMA_i is the individual HOMA-IR index; HOMA_{lean} is the population mean of HOMA-IR index for lean population; EFF_{HOMA} is the parameter of the covariate relationship; k_{tra} is the typical value of conversion rate constant for chylomicron to VLDL-V6; η_i is individual deviation from k_{tra} ; a random effect belonging to a distribution with mean zero and standard deviation ω_{ktra} .

or very obese. Although other studies have investigated the postprandial response of these measures, this study evaluated the biomarkers for an extended duration after the meal. Our work shows a differential regulation of glucose homeostasis and lipid metabolism between the lean and the obese or very obese populations. Additionally, the clinical data were utilized to develop an integrated semimechanistic model of TGs, insulin, glucose, and active GLP-1 (the TIGG model). The TIGG model was able to describe the postprandial responses in individuals who are lean, obese, and very obese and elucidate the complex relationship between these biomarkers despite the use of a parsimonious modeling approach.

Consistent with the literature, the very obese population had an impaired postprandial response compared to lean or obese.^{26,27} The iAUC of active GLP-1 was significantly lower in individuals who are very obese compared with both individuals who are obese or lean. Previous GLP-1 modeling had associated the postprandial GLP-1 changes to the predicted glucose amount within the small intestine, peaking around 45 minutes, and returning to baseline 2 hours postmeal.²⁸ Within this clinical data, the first postmeal sample was collected at 4 hours and active GLP-1 levels were elevated for all populations. Given this, the intestinal glucose could not be the only driver of GLP-1 response. Additionally, the major nutrient within the test meal was fat instead of glucose. Both active GLP-1 and TGs in chylomicrons and VLDL-V6 had an apparent postprandial peak at 4 hours postmeal. As oral intake of fat increased GLP-1 secretion in a dose-dependent manner,^{13,29–31} the TGs in the transit compartments, chylomicrons, and VLDL-V6 were investigated in the TIGG model as drivers for the postprandial active GLP-1 response. Interestingly, the TGs in the second transit compartment (representing intestinal TGs) provided the better fit and aligned biologically, as GLP-1 is mainly derived from the gut.

The observed insulin concentrations peaked at 4 hours postmeal for all study populations. However, postprandial increases in glucose were not observed in any of the study populations. This is likely reflective of the lack of samples collected between 0 and 4 hours postmeal, as a postprandial peak should occur ~1–2 hours postmeal after consumption of ~30 g of carbohydrates.²³ Furthermore, the temporal response between insulin and glucose was not observed within the study for any of the

populations. Although surprising, this has been observed by others as well. Shah *et al.*³² observed that insulin concentrations remained elevated 3 hours postmeal, whereas glucose levels had returned to premeal concentration 1 hour after consuming either a high-protein or high-fat meal in individuals who are overweight/obese. Within the IGI model, insulin secretion is driven by the glucose ratio between dynamic and steady-state glucose (ratio of change in glucose). The observed glucose concentration remained flat at euglycemic levels throughout the entire collected 13-hour postprandial assessment period in the lean population. Therefore, the glucose ratio equaled 1 for the lean population within this study, resulting in no insulin secretion in the IGI model. Instead, the changes in insulin were associated with active GLP-1 which was elevated at 4 hours postmeal, as it is well-established that GLP-1 increases insulin secretion.^{33,34}

Insulin resistance is associated with adiposity and is due to an increase in glucose production, as well as a reduction in peripheral glucose disposal.^{25,35} Correspondingly, fasting insulin concentrations differed among the lean, obese, and very obese populations, increasing incrementally in the obese and very obese populations compared with lean. To account for this physiological difference in the TIGG model, different insulin baselines were estimated for each population, reflecting the different insulin secretion rates.³⁶ Insulin-dependent glucose clearance, representing the majority of glucose disposal for elevated insulin, was also adjusted in the model using the fasting insulin ratio between the obese or very obese populations to the lean. Elevated fasting insulin concentrations in the obese or very obese populations relative to lean would result in a decrease of the insulin-dependent glucose clearance and reflect impaired peripheral glucose disposal. Fasting glucose concentrations were significantly elevated in the obese and very obese compared with the lean population. Accordingly, different glucose baselines were estimated for each population. Likewise, glucose production was also adjusted using the relative change in fasting glucose concentration between the obese or very obese populations, in relation to the lean. Thus, elevated fasting glucose in the obese and very obese populations would reflect both a greater glucose production and a reduction in glucose disposal via insulin-dependent glucose clearance.

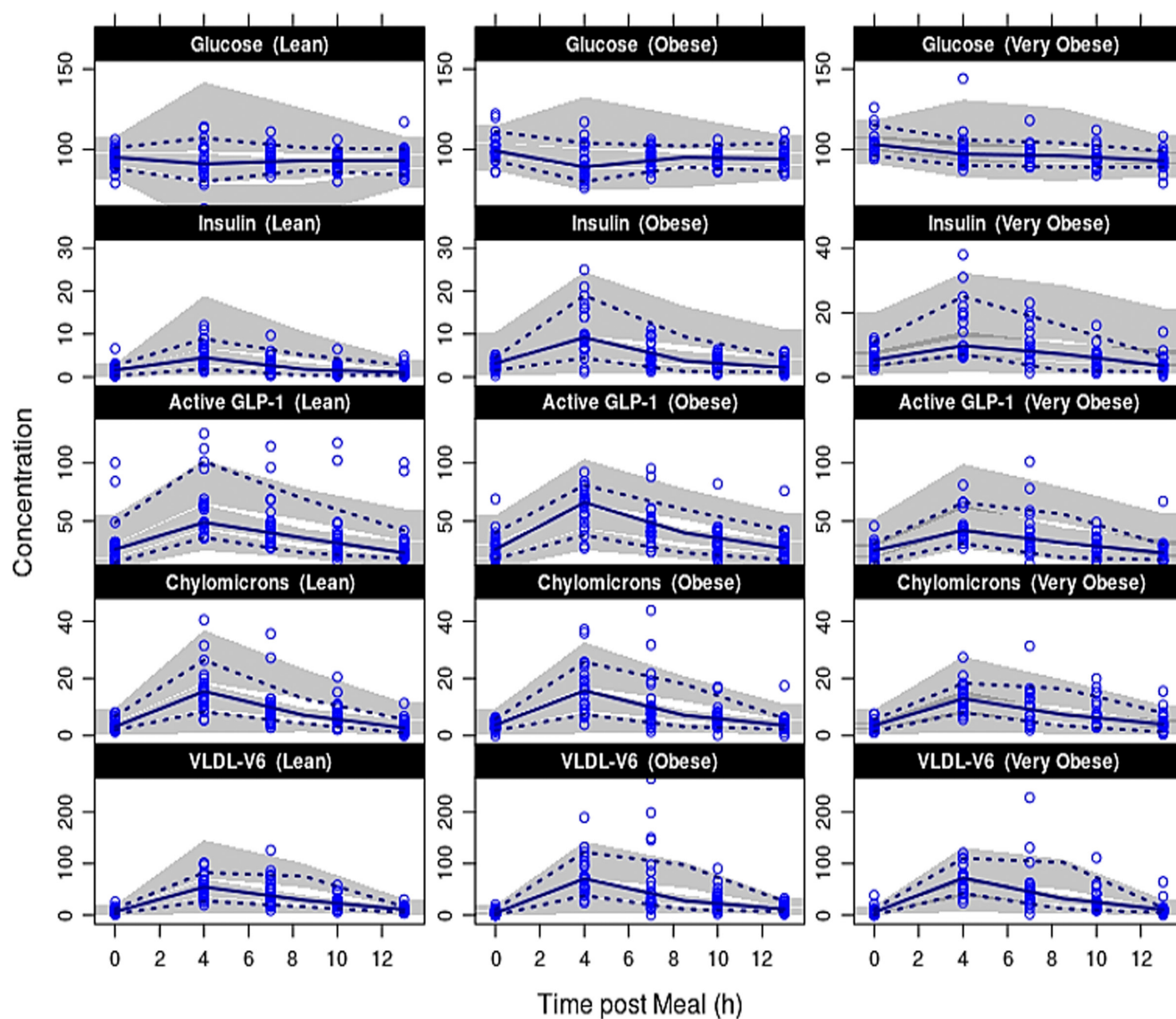


Figure 3 Visual predictive check of the model predictions of glucose (top row), insulin (second row), active GLP-1 (third row), chylomicron concentration (fourth row), and VLDL-V6 concentrations (bottom row) for the three investigated populations lean (left column), obese (middle column), and very obese (right column). The blue symbols are observation related: dots are observations, solid line is median, and dashed line is the 10th and 90th percentile of data. The grey shaded area represents the 80% CI of the 10th, 50th, and 90th percentiles of model simulations. CI, confidence interval. [Colour figure can be viewed at wileyonlinelibrary.com]

Differences in glucose homeostasis among lean, obese, and very obese populations were observed during the extended postprandial period. In the lean population, the observed glucose concentration remained euglycemic during the entire collected postprandial assessment period of 13 hours. In contrast, the obese and very obese populations had elevated fasting glucose which diminished during the postprandial period until they achieved euglycemia within 4 and 13 hours postmeal, respectively. To our knowledge, this phenomenon has not been previously reported as most studies investigate shorter postprandial periods. The data suggest a difference in glucose homeostasis between the lean population and the obese or very obese during an extended fasting period after a meal. These differences were substantiated during model development. When fixing the

glucose-independent and glucose-dependent clearance to the healthy populations' parameters of the IGI model, the model was unable to describe the glucose profile of the lean population. The model predicted that glucose should be reduced due to elevated postprandial insulin. However, unfixing the insulin-dependent glucose clearance resulted in a zero estimate, which is physiologically impossible. This inferred that either glucose production had to be increased or peripheral glucose disposal had to be reduced to maintain euglycemia observed in lean individuals. Importantly, the model-predicted glucose profile for the obese and very obese populations reflected the observed data, unlike the lean population.

Greater peripheral glucose disposal is typically observed in the lean population compared with the obese who can have peripheral

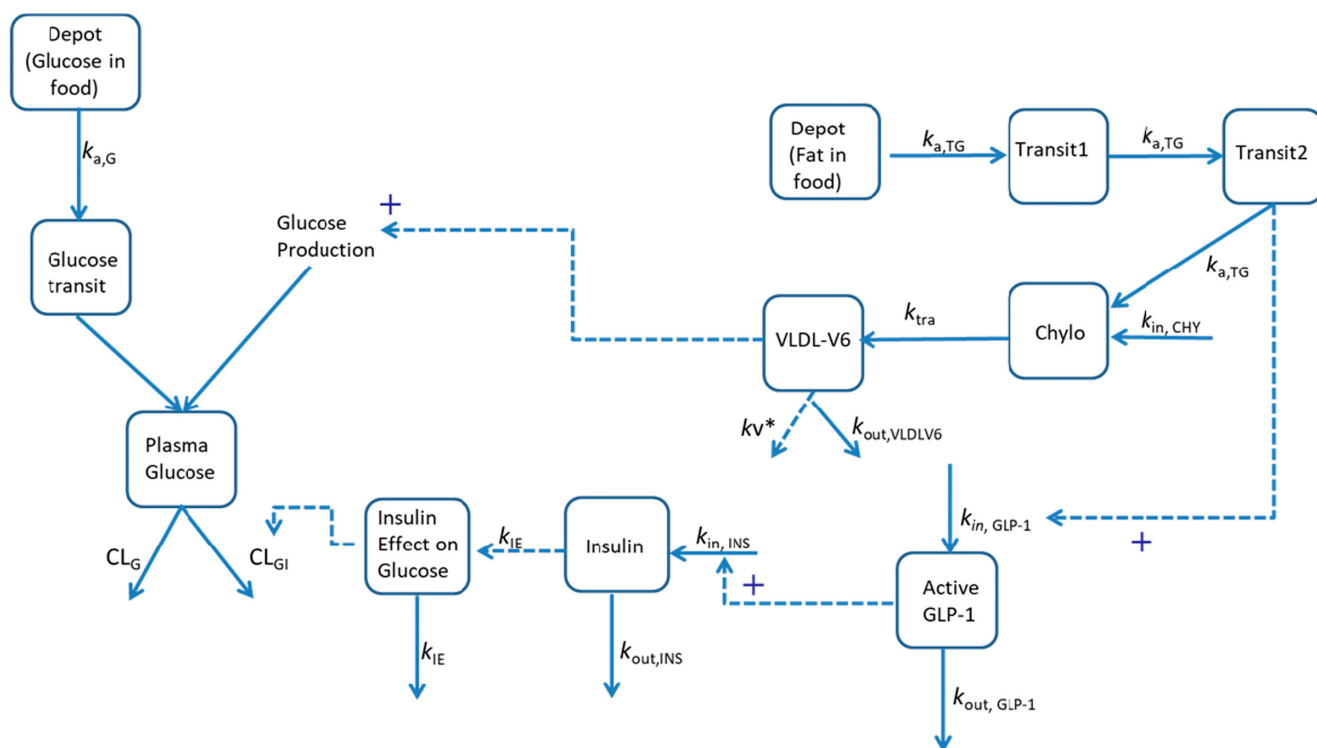


Figure 4 Schematic representation of the model. CL_G , insulin-independent glucose clearance; CL_{GI} , insulin-dependent glucose clearance; $k_{a,G}$, absorption rate constant for glucose; k_{IE} , rate constant for insulin delay; $k_{a,TG}$, absorption rate constant for triglycerides; $k_{in,CHY}$, rate constant of production of chylomicron; $k_{in,GLP1}$, rate constant of production of active GLP-1; $k_{in,GNS}$, rate constant of production of insulin; k_{tra} , conversion rate constant for chylomicron to VLDL-V6; $k_{out,GLP1}$, first order rate constant for the elimination of active GLP1; $k_{out,INS}$, first order rate constant for the elimination of insulin; $k_{out,VLDLV6}$, first order rate constant for the elimination of VLDL-V6; kv^* , net zero order rate constant for the elimination of VLDL-V6. [Colour figure can be viewed at wileyonlinelibrary.com]

insulin resistance. Additionally, higher energy expenditure has been noted in lean individuals compared with individuals who are overweight.³⁷ Given these observations, one possibility is that another fuel source is used to preserve euglycemia in individuals who are lean. In the postmeal state, oxidation of FFAs sustains the energy needs for most of the body, which competes with glucose in certain organs.³⁸ Importantly, it has also been shown that normal weight individuals (lean) have the ability to alter fuel substrates in the postprandial state based on what is provided in the meal; whereas, this ability is impaired in individuals who are obese.³⁶ Correspondingly, after a high-fat meal, higher lipid oxidation is observed in individuals who are lean compared with obese.³⁷

Chylomicrons and VLDL deliver FFAs to the heart, skeletal muscle, and adipose tissue for energy expenditure and storage.³⁹ An increase in lipid oxidation would reduce the amount of glucose needed to maintain the energy expenditure requirement. Additionally, when TGs are hydrolyzed, they release FFAs and the byproduct of glycerol, which can be converted to glucose in the liver. The effect of increasing endogenous glucose production using either the TGs in chylomicrons or VLDL-V6 was investigated within the TIGG model and using the TGs in VLDL-V6 explained the observed glucose data. Correspondingly, postprandial TG excursions in VLDL-V6 were lower in the lean population compared with the obese or very obese, likely reflecting greater lipid oxidation. With this addition to the model, glucose profiles

were well captured for all study populations. The model revealed that the lean population sustain euglycemia by utilizing more of the TGs in VLDL-V6 for lipid oxidation than the obese, thereby reducing the amount of glucose needed to maintain the energy expenditure requirements in the extended period after the meal.

This TIGG model provides an advancement over the other existing models, but development was performed using a relatively small clinical study with homogeneous ethnicity and racial background. Further studies will be needed to confirm our findings across various racial, ethnic backgrounds, and disease states. This study used a high fat test meal with a fixed amount of carbohydrate, fats, and protein. Further model development would be needed for other types of meals containing different meal compositions. Additionally, this model does not include FFAs, an important component for the description of the TG dynamics within the body. Further, collecting samples prior to 4 hours would allow for the characterization of the initial postprandial glucose response which was missing within this study.

CONCLUSIONS

This work demonstrated a differential regulation of glucose homeostasis and lipid metabolism between the lean population to the obese or very obese. The developed TIGG model was able to characterize and quantify the response following a high-fat meal in individuals who are lean, obese, and very obese and provide insight into the possible regulation of glucose homeostasis in

extended fasting after meal. The TIGG model is the first model to integrate the glucose and insulin regulation, incretin effect, along with postprandial TG response in chylomicrons and VLDL-V6 in a semimechanistic way.

SUPPORTING INFORMATION

Supplementary information accompanies this paper on the *Clinical Pharmacology & Therapeutics* website (www.cpt-journal.com).

ACKNOWLEDGMENTS

The authors would like to thank Dr. Jeffrey Suico who was the principal investigator for this study, Amanda Cantrell who was the clinical pharmacology manager and provided clinical trial oversight, and Hollins Showalter who provided statistical support.

FUNDING

This study was supported by Eli Lilly and Company.

CONFLICTS OF INTEREST

J.L. is an employee and minor stockholders in Eli Lilly and Company. M.K. declared no competing interests for this work.

AUTHOR CONTRIBUTIONS

J.L. and M.K. designed and performed research. J.L. analyzed the data. J.L. and M.K. wrote the manuscript.

DATA AVAILABILITY STATEMENT

The data are not publicly available due to privacy or ethical restrictions. The data that support the findings of this study are available on request from the corresponding author. Access is provided after a proposal has been approved by an independent review committee identified for this purpose and after receipt of a signed data sharing agreement.

© 2022 Eli Lilly and Co. *Clinical Pharmacology & Therapeutics* published by Wiley Periodicals LLC On behalf of American Society for Clinical Pharmacology and Therapeutics.

This is an open access article under the terms of the [Creative Commons Attribution-NonCommercial-NoDerivs](https://creativecommons.org/licenses/by-nc-nd/4.0/) License, which permits use and distribution in any medium, provided the original work is properly cited, the use is non-commercial and no modifications or adaptations are made.

- Malnick, S.D.H., Knobler, H. The medical complications of obesity. *QJM Int. J. Med.* **99**, 565–579 (2006).
- Grundy, S.M. et al. Definition of metabolic syndrome: report of the National Heart, Lung, and Blood Institute/American Heart Association conference on scientific issues related to definition. *Circulation* **109**, 433–438 (2004).
- Højlund, K. Metabolism and insulin signaling in common metabolic disorders and inherited insulin resistance. *Dan. Med. J.* **61**, B4890 (2014).
- Silber, H.E., Jauslin, P., Frey, N., Gieschke, K., Simonsson, U.S. & Karlsson, M.O. An integrated model for glucose and insulin regulation in healthy volunteers and Type 2 diabetic patients following intravenous glucose provocations. *J. Clin. Pharmacol.* **46**, 1159–1171 (2007).
- Jauslin, P.M., Karlsson, M.O. & Frey, N. Identification of the mechanism of action of a glucokinase activator from oral glucose tolerance test data in type 2 diabetic patients based on an integrated glucose-insulin model. *J. Clin. Pharmacol.* **52**, 1861–1871 (2012).
- Schneck, K.B., Zhang, X., Bauer, R., Karlsson, M.O. & Sinha, V.P. Assessment of glycemic response to an oral glucokinase activator in a proof of concept study: application of a semi-mechanistic, integrated glucose-insulin-glucagon model. *J. Pharmacokinet. Pharmacodyn.* **40**, 67–80 (2013).
- Zhang, X., Schneck, K., Bue-Valleskey, J., Yeo, K.P., Heathman, M. & Sinha, V. Dose selection using a semi-mechanistic integrated glucose-insulin-glucagon model: designing phase 2 trials for a novel oral glucokinase activator. *J. Pharmacokinet. Pharmacodyn.* **40**, 53–65 (2013).
- Felig, R. & Wahren, J.C. Fuel homeostasis in exercise. *N. Engl. J. Med.* **293**, 1078–1084 (1975).
- Marliss, E.B. & Vranic, M. Intense exercise has an unique effects on both insulin release and its role on glucoregulation. *Diabetes* **51**, S271–S283 (2002).
- Leohr, J., Heathman, M. & Kjellsson, M.C. Semi-physiological model of postprandial triglyceride response in lean, obese and very obese individuals after a high-fat meal. *Diabetes Obes. Metab.* **20**, 660–666 (2018).
- Nakajima, K. et al. Postprandial lipoprotein metabolism: VLDL vs chylomicrons. *Clin. Chim. Acta.* **412**, 1306–1318 (2011).
- Lucero, D. et al. Predominance of large VLDL particles in metabolic syndrome, detected by size exclusion liquid chromatography. *Clin. Biochem.* **45**, 293–297 (2012).
- Fernández-García, J.C., Murri, M., Coin-Aragüez, L., Alcaide, J., El Bekay, R. & Tinahones, F.J. GLP-1 and peptide YY secretory response after fat load is impaired by insulin resistance, impaired fasting glucose and type 2 diabetes in morbidly obese subjects. *Clin. Endocrinol. (Oxf)* **80**, 671–676 (2014).
- Blackburn, P. et al. Postprandial hyperlipidemia: another correlate of the “hypertriglyceridemic waist” phenotype in men. *Atherosclerosis* **171**, 327–336 (2003).
- Otvos, J., Jeyarsjah, E. & Bennett, D. Quantification of plasma lipoproteins by proton nuclear magnetic resonance spectroscopy. *Clin. Chem.* **37**, 337–386 (1991).
- Jauslin, P.M. et al. An integrated glucose-insulin model to describe oral glucose tolerance test data in type 2 diabetics. *J. Clin. Pharmacol.* **47**, 1244–1255 (2007).
- Elliot, R.M., Morgan, L.M., Tredger, J.A., Deacon, S., Wright, J. & Marks, V. Glucagon-like peptide-1 (7–36)amide and glucose-dependent insulinotropic polypeptide secretion in response to nutrient ingestion in man: acute post-prandial and 24-h secretion patterns. *J. Endocrinol.* **138**, 159–166 (1993).
- Meier, J.J. et al. Secretion, degradation, and elimination of glucagon-like peptide 1 and gastric inhibitory polypeptide in patients with chronic renal insufficiency and healthy control subjects. *Diabetes* **53**, 654–662 (2004).
- Beal, S.L. & Sheiner, L.B. *NONMEM Users Guides* (GloboMax Inc, Hanover, MD, 1989–1998).
- Lindbom, L., Ribbing, J. & Jonsson, E.N. Perl-speaks-NONMEM (PsN)—a Perl module for NONMEM related programming. *Comput. Meth. Prog. Biomed.* **75**, 85–94 (2004).
- Hooker, A.C., Staats, C.E. & Karlsson, M.O. Conditional weighted residuals (CWRES): a model diagnostic for the FOCE method. *Pharm. Res.* **24**, 2187–2197 (2007).
- Jonsson, E.N. & Karlsson, M.O. Xpose—an S-PLUS based population pharmacokinetic/pharmacodynamic model building aid for NONMEM. *Comput. Meth. Prog. Biomed.* **58**, 51–64 (1999).
- Jauslin, P.M., Frey, N. & Karlsson, M.O. Modeling of 24-hour glucose and insulin profiles of patients with type 2 diabetes. *J. Clin. Pharmacol.* **51**, 153–164 (2011).
- Ålskär, O. et al. Semimechanistic model describing gastric emptying and glucose absorption in healthy subjects and patients with type 2 diabetes. *J. Clin. Pharmacol.* **56**, 340–348 (2016).
- Bock, G. et al. Contribution of hepatic and extrahepatic insulin resistance to the pathogenesis of impaired fasting glucose: role of increased rates of gluconeogenesis. *Diabetes* **56**, 1703–1711 (2007).
- Carr, R.D. et al. Secretion and dipeptidyl peptidase-4-mediated metabolism of incretin hormones after a mixed meal or glucose ingestion in obese compared to lean, nondiabetic men. *J. Clin. Endocrinol. Metab.* **95**, 872–878 (2010).
- Verdich, C., Toubro, S., Buemann, B., Lysegård Madsen, J., Juul Holst, J. & Astrup, A. The role of postprandial releases of insulin and incretin hormones in meal-induced satiety—effect of obesity and weight reduction. *Int. J. Obes. Relat. Metab. Disord.* **25**, 1206–1214 (2001).
- Røge, R.M. et al. Mathematical modelling of glucose-dependent insulinotropic polypeptide and glucagon-like peptide-1 following

- ingestion of glucose. *Basic Clin. Pharmacol. Toxicol.* **121**, 290–297 (2017).
29. Tolhurst, G., Reimann, F. & Gribble, F.M. Nutritional regulation of glucagon-like peptide-1 secretion. *J. Physiol.* **587**, 27–32 (2009).
 30. Ballantyne, G.H. Peptide YY(1–36) and peptide YY (3–36): Part I. Distribution, release and actions. *Obes. Surg.* **16**, 651–658 (2006).
 31. Yoder, S.M., Yang, Q., Kindel, T.L. & Tso, P. Stimulation of incretin secretion by dietary lipid: is it dose dependent? *Am. J. Physiol. Gastrointest. Liver Physiol.* **297**, G299–G305 (2009).
 32. Shah, M. *et al.* Effect of meal composition on postprandial glucagon-like peptide-1, insulin, glucagon, C-peptide, and glucose responses in overweight/obese subjects. *Eur. J. Nutr.* **56**, 1053–1062 (2017).
 33. Jones, B., Bloom, S.R., Buenaventura, T., Thomas, A. & Rutter, G. Control of insulin secretion by GLP-1. *Peptides* **100**, 75085 (2018).
 34. Salehi, M., Aulinger, B., Prigeon, R.L., D'Alessio, D.A. Effect of endogenous GLP-1 on insulin secretion in type 2 diabetes. *Diabetes* **59**, 1330–1337 (2010).
 35. Basu, R. *et al.* Pathogenesis of prediabetes: role of the liver in isolated fasting hyperglycemia and combined fasting and postprandial hyperglycemia. *J. Clin. Endocrinol. Metab.* **98**, E409–E417 (2013).
 36. van Vliet, S. *et al.* Obesity is associated with increased basal and postprandial β -cell insulin secretion even in the absence of insulin resistance. *Diabetes* **69**, 2112–2119 (2020).
 37. Adamska-Patruno, E. *et al.* Evaluation of energy expenditure and oxidation of energy substrates in adult males after intake of meals with varying fat and carbohydrate content. *Nutrients* **10**, 627 (2018).
 38. Gerich, J.E. Physiology of glucose homeostasis. *Diabetes Obes. Metab.* **2**, 345–350 (2002).
 39. Klop, B., Elte, J.W.F. & Cabezas, M.C. Dyslipidemia in obesity: mechanisms and potential targets. *Nutrients* **5**, 1218–1240 (2013).